Journal of Chemical Health Risks

www.jchr.org

JCHR (2024) 14(3), 879-898 | ISSN:2251-6727

A Paradigmatic Approach for Physico-Chemical Characterization of COVID-19 Drugs via ST-Polynomial

Lakhdar Ragoub [1], K. Pattabiraman[2], Mohammad Usman Ghani[3], Mohammad Reza Farahani [4], Mehdi Alaeiyan[4], Murat Cancan[5]

[1] Mathematics Department, University of Prince Mugrin, P.O. Box 41040, 42241 Al Madinah, Saudia Arabia.

[2] Department of Mathematics Government Arts College (Autonomous) Kumbakonam 612 001, India.

[3] Institute of Mathematics, Khawaja Fareed University of Engineering & Information Technology, Abu Dhabi Road, 64200, Rahim Yar Khan, Pakistan

[4]Department of Mathematics and Computer Science,In University of Science and Technology (IUST), Narmak, Tehran, 16844, Iran.

[5]Faculty of Education, Van Yuzuncu Yl University, Zeve Campus, 65080, Van, Turkey

(Received: 04 February 2024 Revised: 11 March 2024 Accepted: 08 April 2024)

KEYWORDS

COVID-19, Quantitative Structure-Property Relationship (QSPR), ST-Polynomial, Topological indices of molecular graph COVID-19

ABSTRACT:

One of the most infectious diseases in recorded human history, Coronavirus Disease-19 (COVID-19), is a severe acute respiratory syndrome coronavirus 2 (SARS-CoV-2)-related illness that has already claimed millions of lives throughout the globe. Neither vaccines nor effective medicines are currently available that can effectively treat COVID-19 patients or stop the virus's transmission. The development of medications and vaccinations may take a long time, but scientific communities all around the world have responded quickly and have been working nonstop on them. Repurposing the already available antiviral medications may be the best course of action in the face of this uncertainty to hasten the development of efficient treatments for SARS-CoV-2. Drug repurposing may also provide important information on druggable targets, which might be used to develop new drugs using a target-based approach. Updated information is also required on potential pharmacological targets, therapeutic and vaccine development, and results. The design and analysis of approximation techniques for graph partitioning issues, the investigation of random walks in graphs, and the creation of expander graphs are all applications of spectral graph theory. For numerous COVID-19 antiviral medications, we suggest status distance-based polynomials and topological descriptors in this work. We also examine the suggested topological indices' Quantitative Structure-Property Relationship (QSPR). Curve fitting models for the physico-chemical properties of the COVID-19 drugs are obtained and looked at in line with the specified indices. Our models and results may facilitate the development of innovative drugs for the treatment of COVID-19.

1. Introduction

As of June 30, 2020, there were 10,421,869 confirmed cases of COVID-19 (Figure 1), which initially appeared in China. There were also 508,422 confirmed fatalities (worldometers.info/coronavirus/). COVID-19 and earlier epidemics like SARS and the Middle East Respiratory Syndrome (MERS), in addition to sharing comparable signs and symptoms like a sore throat, a persistent high fever, and pneumonia, also share similar pathologies including immune dysfunction and multi-organ failure (Andersen, Rambaut, Lipkin, Holmes, & Garry, 2020; Forster, Forster, Renfrew, & Forster,

Journal of Chemical Health Risks
www.jchr.org
JCHR (2024) 14(3), 879-898 | ISSN:2251-6727

2020). Like other coronaviruses, SARSCoV-2 has a variety of structural and non-structural proteins that are essential to cellular functions (Ashour, Elkhatib, Rahman, &Elshabrawy, 2020). Spike glycoproteins are among the structural proteins that help the virus adhere to its host cells. The non-structural proteins necessary for viral replication include the helicase, major protease (Mpro), papain-like protease (PLpro), and RNA dependent RNA polymerase (RdRp) (Forster et al., 2020; Siu et al., 2008). These proteins provide intriguing pharmacological targets for creating possible therapeutics against SARS-CoV-2 infection because of their essential involvement in the viral life cycle.

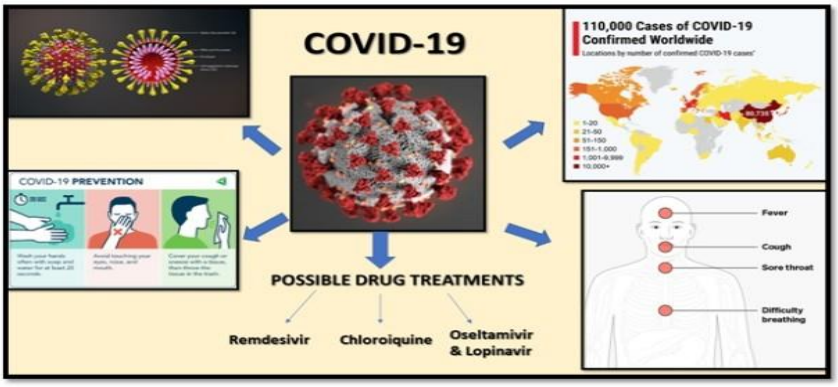

Figure 1. The resulting infectious disease was referred to by the World Health Organization as Corona virus 2019 (COVID-19).

Although the scientific community has moved quickly, COVID-19 currently has no vaccine or viable treatments (Figure 2) (Harrison, 2020). Remdesivir is one of the antiviral medications now on the market that has been used to treat different viral infections. This treatment for COVID-19 patients has had conflicting results (Gautret et al., 2020; Molina et al., 2020). So, it is essential to concentrate on alternate, logical approaches for the creation of urgent treatments to stop the epidemic.

Understanding the sickness, the immune response after infection, and the pathophysiology of the virus is necessary for the development of novel treatment medications and vaccines. We thoroughly evaluate all pertinent published research on this topic in order to produce a scoping review that summarises the prospective pharmacological targets and treatments now undergoing trials in order to speed up this endeavour. This evaluation would offer verifiable proof of the drug targets, drug usage in the past and early indications of potential pharmacological mechanisms. Our assessment would also offer useful data for further SARS-CoV-2 research and might help researchers find a suitable treatment, see Figure 3.

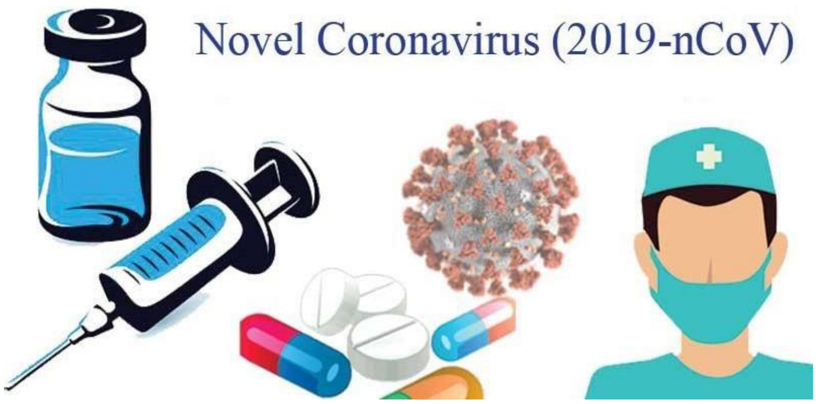

Figure 2. Updates on treatment and vaccine for novel coronavirus (2019-nCOV).

Journal of Chemical Health Risks

www.jchr.org

JCHR (2024) 14(3), 879-898 | ISSN:2251-6727

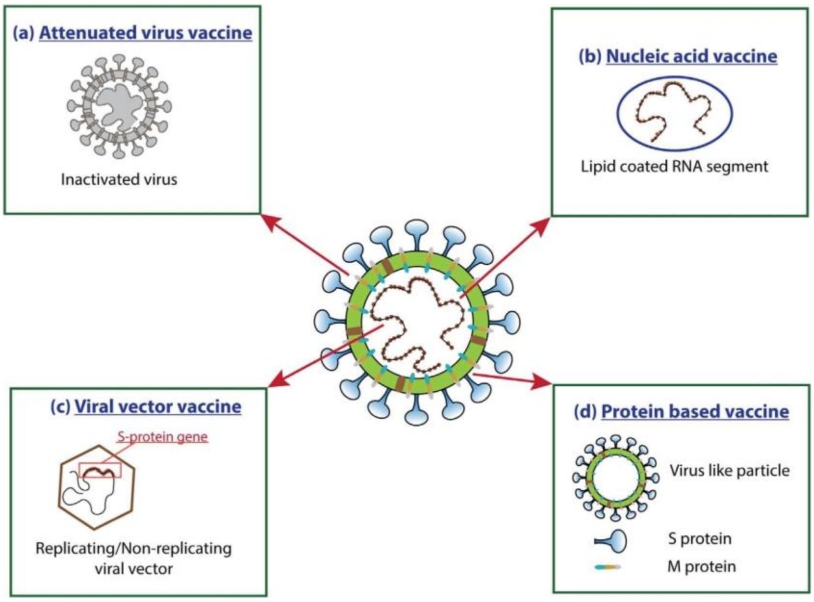

Figure 3. Possible strategies for vaccine design and development.

The mathematical discipline known as chemical graph theory focuses on chemical graphs, which are pictures of chemical systems. Chemical graph theory is used in the development of topological indices for COVID-19 medicines. Topological Indices (TIs), which are generated from molecular graphs, are numerical descriptors used to characterise chemical systems. They are mostly used to investigate the physiochemical properties of different drugs. Chemical graph theory relies heavily on the intricate computation of a wide variety of polynomial types and topological indices, which show chemical structure. The importance of status distance-based topological indices in these classes, and chemistry in particular, cannot be overstated. In QSPR and QSAR research, graph invariants (TIs) have garnered a lot of attention in recent years. The most important applications of the topological indices to date are the non-empirical Quantitative Structure-Property Relationships (QSPR) and Quantitative Structure-Activity Relationships (QSAR) [4, 5, 6, 34-49].

Numerous fields, including biology, mathematics, bioinformatics, informatics, and others, have used topological indices in their research. The QSPR models establish how topological indices and psychochemical characteristics should be related. These psychochemical features are being studied because they have a substantial impact on drug transit and bioactivity in the human body. In this work, we compute the status distance-based TIs linked to the COVID-19 indicated drugs. Similar to this, COVID-19 medicines are an example of a chemical substance for which the specified topological indices are well defined and included in QSPR analysis. The equivalent characteristic determined in this manner has a significant connection with the characteristic of COVID-19 medicines using the curve fitting technique.

Material and Method

Let G=(V, E) be a molecular graph with the vertex set V=V(G) and the edge set E=E(G). A molecular graph is a straightforward finite graph where the edges represent chemical bonds and the vertices represent atoms [11] is a general source for the notation used in graph theory. The length of the shortest path (the number of edges in it) connecting the vertices u and v of the graph G is equal to the distance d(u,v) between them. Two vertices u and v are connected by an edge e=uv of the graph G (d(u,v)=1).The status [26] of a vertex v in G is the sum of the distance from v to all other vertices in G, that is

$$s_v = \sum_{u \in V} d(u,v)$$

In [27-32], status-distance based TIs are examined in terms of their mathematical properties and chemical applications. In the literature, a number of graph polynomials were introduced, and some of them proved to be beneficial in mathematical chemistry. Graph

Journal of Chemical Health Risks

www.jchr.org

JCHR (2024) 14(3), 879-898 | ISSN:2251-6727

polynomials are functions of isomorphism-invariant graphs. Usually, they are polynomials with integer coefficients in one or two variables. Because some subgraphs are virtually always counted, graph polynomials can be thought of as regular generating functions for the sequences of coefficients. In the field of distance-based topological indices, the Hosoya polynomial [12] is an important polynomial; see also [13-15]. With an evaluation of 1, the Hosoya polynomial's first derivative can be used to derive the Wiener index [33]. Domination polynomials, chromatic polynomials, independence polynomials, matching polynomials, Tutte polynomials, reliability polynomials, characteristic polynomials, subgraph polynomials, clique polynomials, forest polynomials, Padmakar-Ivan polynomials, and Omega polynomials are a few notable examples of graph polynomials. See [7-10, 16-25] for a definition of these polynomials.

In 2015, Klavzar and Deutsch published the M-polynomial, a degree-based invariants polynomial [25]. They demonstrate that the functions for degree-based invariants and distance-based invariants of the Hosoya polynomial are equal.

In accordance with polynomials studied previously, we introduce new polynomial called ST-Polynomial (ST_P) with respect to status distance of a graph G which is defined as

$ST(G,x,y) = \sum_{i \le j} d_{ij} x^i y^j$, where

$d_{ij} = \{ |E_{ij}| \, | \, \{ s_u = i, s_v = j \} \}$.

TIs based on the vertex status distance is defined as

$STI(G) = \sum_{uv \in E} h(s_u, s_v)$ ------------------------------------(1)

The following operators are used in **Table 1**

$$s_x = x\left(\frac{\partial (h(x,y))}{\partial x}\right),$$

$$s_y = y\left(\frac{\partial (h(x,y))}{\partial y}\right),$$

$$E_x = \int_0^x \frac{h(t,y)}{t} dt,$$

$$E_y = \int_0^y \frac{h(x,t)}{t} dt,$$

$$c_k(h(x,y)) = x^k h(x,y)$$

and $J(h(x,y)) = h(x,x)$. If $m_u = s_u$ and $m_v = s_v$ then we have $h(x,y) = ST(G,x,y)$.

Table 1. Topological indices and their mathematical formulations.

Topological indices	Mathematical Expressions (m_u, m_v)	Derivation from $ST(G,x,y)$
First status connectivity index $\mathbf{S_1}$ [28,30]	$\sum_{uv \in E} (m_u + m_v)$	$((s_x + s_y)h(x,y))(1,1)$
Second status connectivity $\mathbf{S_2}$ [28,30]	$\sum_{uv \in E} m_u m_v$	$((s_x s_y)h(x,y))(1,1)$
Inverse second status connectivity index $\mathbf{S_3}$	$\sum_{uv \in E} \frac{1}{m_u m_v}$	$((E_x E_y)h(x,y))(1,1)$
Forgotten status index **FS**	$\sum_{uv \in E} (m_u^2 + m_v^2)$	$((s_x^2 + s_y^2)h(x,y))(1,1)$
Reformulated status index **RS**	$\sum_{uv \in E} m_u m_v (m_u + m_v)$	$((s_x s_y (s_x + s_y))h(x,y))(1,1)$

Journal of Chemical Health Risks

www.jchr.org

JCHR (2024) 14(3), 879-898 | ISSN:2251-6727

Symmetric deg division status index **SDDS**	$\sum_{uv\in E}\left(\frac{\mu_u}{\mu_v}+\frac{\mu_v}{\mu_u}\right)$	$\left(\left(S_xE_y+E_xS_y\right)h(x,y)\right)(1,1)$
Inverse sum indeg status index **ISSI**	$\sum_{uv\in E}\left(\frac{\mu_u\mu_v}{\mu_u+\mu_v}\right)$	$\left(\left(E_xJS_xS_y\right)h(x,y)\right)(1)$
Harmonic Status index **HS** [29]	$\sum_{uv\in E}\left(\frac{2}{\mu_u+\mu_v}\right)$	$\left(\left(2E_xJ\right)h(x,y)\right)(1)$
Augmented status index **AS**	$\sum_{uv\in E}\left(\frac{\mu_u\mu_v}{\mu_u+\mu_v-2}\right)^3$	$\left(\left(E_x^3\chi_{-2}JS_x^3S_y^3\right)h(x,y)\right)(1)$

3.STp for Covid drugs

In this section, we find the ST-polynomials for six antiviral drugs used in the treatment of COVID-19 such as lopinavir-d8 (CID71749833) which is ritonavir analog, CID89869520 structure which is favipiravir analog, CID10009410, CID44271905, CID3010243 and CID271958 structures which are structural analog of lopinavir. These structures have the property of being potential drugs against COVID-19. Using these polynomials, various TIs depending on the status distance are calculated for these drugs.

Theorem 3.1.1. Let G_1 be the chemical graph of CID71749833 structure. Then

$$\begin{aligned}ST(G_1,x,y) = {} & x^{281}y^{292} + x^{281}y^{320} + x^{281}y^{286} + x^{286}y^{293} + x^{292}y^{305} + x^{293}y^{344} + x^{293}y^{304} + x^{304}y^{343} \\ & + x^{304}y^{331} + x^{305}y^{322} + x^{305}y^{356} + x^{320}y^{361} + x^{322}y^{357} + x^{322}y^{361} + x^{322}y^{373} + x^{331}y^{360} \\ & + x^{343}y^{384} + 2x^{357}y^{402} + x^{360}y^{411} + x^{360}y^{393} + 3x^{361}y^{408} + x^{361}y^{406} + 2x^{384}y^{431} \\ & + x^{393}y^{428} + 6x^{402}y^{453} + x^{406}y^{453} + x^{406}y^{457} + 3x^{408}y^{455} + x^{428}y^{465} + 2x^{431}y^{478} \\ & + x^{453}y^{500} + x^{455}y^{500} + 2x^{455}y^{502} + 2x^{465}y^{510} + 2x^{478}y^{525} + x^{510}y^{561} + 2x^{510}y^{557} \\ & + x^{557}y^{602}.\end{aligned}$$

Proof. From Figure1, it is easy to see that $|V| = 53, |E| = 56$ and also

$|E_{281,292}| = 1, |E_{281,320}| = 1,$

$|E_{281,286}| = 1, |E_{286,293}| = 1, |E_{292,305}| = 1,$

$|E_{293,344}| = 1, |E_{293,304}| = 1,$

$|E_{304,343}| = 1, |E_{304,331}| = 1,$

$|E_{305,322}| = 1, |E_{305,356}| = 1, |E_{320,361}| = 1, |E_{322,357}| = 1$

$, |E_{322,361}| = 1, |E_{322,373}| = 1, |E_{331,360}| = 1,$

$|E_{343,384}| = 1, |E_{357,402}| = 2, |E_{360,411}| = 1, |E_{360,393}| = 1$

$, |E_{361,408}| = 3, |E_{361,406}| = 1, |E_{384,431}| = 2,$

$|E_{393,428}| = 1, |E_{402,453}| = 6, |E_{406,453}| = 1, |E_{406,457}| = 1$

$, |E_{408,455}| = 3, |E_{428,465}| = 1, |E_{431,478}| = 2,$

$|E_{453,500}| = 1, |E_{455,500}| = 1, |E_{455,502}| = 2, |E_{465,510}| = 2,$

$|E_{478,525}| = 2, |E_{510,561}| = 1, |E_{510,557}| = 2,$

$|E_{510,561}| = 1, |E_{557,602}| = 2.$

From the Equation (1), it is obtained

$$
\begin{aligned}
ST(G_1,x,y) = {} & \sum_{281\le 292} d_{281,292}x^{281}y^{292} + \sum_{281\le 320} d_{281,320}x^{281}y^{320} \\
& + \sum_{281\le 286} d_{281,286}x^{281}y^{286} + \sum_{286\le 293} d_{286,293}x^{286}y^{293} \\
& + \sum_{292\le 305} d_{292,305}x^{292}y^{305} + \sum_{293\le 344} d_{293,344}x^{293}y^{344} \\
& + \sum_{453\le 500} d_{453,500}x^{453}y^{500} + \sum_{455\le 500} d_{455,500}x^{455}y^{500} \\
& + \sum_{455\le 502} d_{455,502}x^{455}y^{502} + \sum_{465\le 510} d_{465,510}x^{465}y^{510} \\
& + \sum_{478\le 525} d_{478,525}x^{478}y^{525} + \sum_{510\le 561} d_{510,561}x^{510}y^{561} \\
& + \sum_{510\le 561} d_{510,561}x^{510}y^{557} + \sum_{557\le 602} d_{557,602}x^{557}y^{602}. \\
& + \sum_{293\le 304} d_{293,304}x^{293}y^{304} + \sum_{304\le 343} d_{304,343}x^{304}y^{343} \\
& + \sum_{304\le 331} d_{304,331}x^{304}y^{331} + \sum_{305\le 322} d_{305,322}x^{305}y^{322} \\
& + \sum_{305\le 356} d_{305,356}x^{305}y^{356} + \sum_{320\le 361} d_{320,361}x^{320}y^{361} \\
& + \sum_{322\le 357} d_{322,357}x^{322}y^{357} + \sum_{322\le 361} d_{322,361}x^{322}y^{361} \\
& + \sum_{322\le 373} d_{322,373}x^{322}y^{373} + \sum_{331\le 360} d_{331,360}x^{331}y^{360} \\
& + \sum_{343\le 384} d_{343,384}x^{343}y^{384} + \sum_{357\le 402} d_{357,402}x^{357}y^{402} \\
& + \sum_{360\le 411} d_{360,411}x^{360}y^{411} + \sum_{360\le 393} d_{360,393}x^{360}y^{393} \\
& + \sum_{361\le 408} d_{361,408}x^{361}y^{408} + \sum_{361\le 406} d_{361,406}x^{361}y^{406} \\
& + \sum_{384\le 431} d_{384,431}x^{384}y^{431} + \sum_{393\le 428} d_{393,428}x^{393}y^{428} \\
& + \sum_{402\le 453} d_{402,453}x^{402}y^{453} + \sum_{406\le 453} d_{406,453}x^{406}y^{453} \\
& + \sum_{406\le 457} d_{406,457}x^{406}y^{457} + \sum_{408\le 455} d_{408,455}x^{408}y^{455} \\
& + \sum_{428\le 465} d_{428,465}x^{428}y^{465} + \sum_{431\le 478} d_{431,478}x^{431}y^{478}
\end{aligned}
$$

$$
\begin{aligned}
ST(G_1,x,y) = {} & x^{281}y^{292} + x^{281}y^{320} + x^{281}y^{286} + x^{286}y^{293} + x^{292}y^{305} + x^{293}y^{344} + x^{293}y^{304} + x^{304}y^{343} \\
& + x^{304}y^{331} + x^{305}y^{322} + x^{305}y^{356} + x^{320}y^{361} + x^{322}y^{357} + x^{322}y^{361} + x^{322}y^{373} + x^{331}y^{360} \\
& + x^{343}y^{384} + 2x^{357}y^{402} + x^{360}y^{411} + x^{360}y^{393} + 3x^{361}y^{408} + x^{361}y^{406} + 2x^{384}y^{431} \\
& + x^{393}y^{428} + 6x^{402}y^{453} + x^{406}y^{453} + x^{406}y^{457} + 3x^{408}y^{455} + x^{428}y^{465} + 2x^{431}y^{478} \\
& + x^{453}y^{500} + x^{455}y^{500} + 2x^{455}y^{502} + 2x^{465}y^{510} + 2x^{478}y^{525} + x^{510}y^{561} + 2x^{510}y^{557} \\
& + x^{557}y^{602}.
\end{aligned}
$$

The 3D chemical structure and 3D plot of the ST_P of **CID71749833** structure are displayed Figure 4.

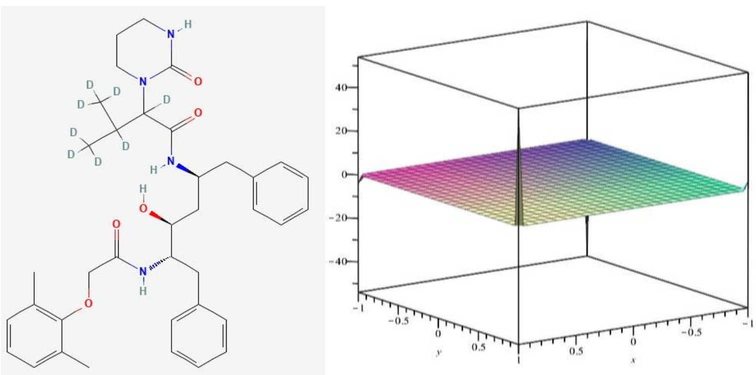

Figure 4. The chemical structure and the Plot of ST_P of **CID71749833** structure.

Journal of Chemical Health Risks
www.jchr.org
JCHR (2024) 14(3), 879-898 | ISSN:2251-6727

Theorem 3.1.2. The G_1 graph's various TIs are as follows:

$S_1(G_1) = 45968$ $\quad SDDS(G_1) = 112.6173684$

$S_2(G_1) = 9736630$. $\quad ISSI(G_1) = 11460.63794$

$S_3(G_1) = 0.000370867$

$HS(G_1) = 0.141375317$ $FS(G_1) = 19578212$

$AS(G_1) = 534864898.3$

$RS(G_1) = 8544281706$

Proof. The following equations are derived from Theorem 3.1.1;

$$\begin{aligned} s_x(ST(G_1,x,y)) = {} & 281x^{281}y^{292} + 281x^{281}y^{320} + 281x^{281}y^{286} + 286x^{286}y^{293} + 292x^{292}y^{305} \\ & + 293x^{293}y^{344} + 293x^{293}y^{304} + 304x^{304}y^{343} + 304x^{304}y^{331} + 305x^{305}y^{322} \\ & + 305x^{305}y^{356} + 320x^{320}y^{361} + 322x^{322}y^{357} + 322x^{322}y^{361} + 322x^{322}y^{373} \\ & + 331x^{331}y^{360} + 343x^{343}y^{384} + 714x^{357}y^{402} + 360x^{360}y^{411} + 360x^{360}y^{393} \\ & + 1083x^{361}y^{408} + 361x^{361}y^{406} + 768x^{384}y^{431} + 393x^{393}y^{428} + 2412x^{402}y^{453} \\ & + 406x^{406}y^{453} + 406x^{406}y^{457} + 1224x^{408}y^{455} + 428x^{428}y^{465} + 862x^{431}y^{478} \\ & + 453x^{453}y^{500} + 455x^{455}y^{500} + 910x^{455}y^{502} + 930x^{465}y^{510} + 956x^{478}y^{525} \\ & + 1020x^{510}y^{561} + 1020x^{510}y^{557} + 1114x^{557}y^{602}. \end{aligned}$$

$$\begin{aligned} s_y(ST(G_1,x,y)) = {} & 292x^{281}y^{292} + 320x^{281}y^{320} + 286x^{281}y^{286} + 293x^{286}y^{293} + 305x^{292}y^{305} \\ & + 344x^{293}y^{344} + 304x^{293}y^{304} + 343x^{304}y^{343} + 331x^{304}y^{331} + 322x^{305}y^{322} \\ & + 356x^{305}y^{356} + 361x^{320}y^{361} + 357x^{322}y^{357} + 361x^{322}y^{361} + 373x^{322}y^{373} \\ & + 360x^{331}y^{360} + 384x^{343}y^{384} + 804x^{357}y^{402} + 411x^{360}y^{411} + 393x^{360}y^{393} \\ & + 1224x^{361}y^{408} + 406x^{361}y^{406} + 862x^{384}y^{431} + 428x^{393}y^{428} + 2718x^{402}y^{453} \\ & + 453x^{406}y^{453} + 457x^{406}y^{457} + 1365x^{408}y^{455} + 465x^{428}y^{465} + 956x^{431}y^{478} \\ & + 500x^{453}y^{500} + 500x^{455}y^{500} + 1004x^{455}y^{502} + 1020x^{465}y^{510} + 1050x^{478}y^{525} \\ & + 1122x^{510}y^{561} + 1114x^{510}y^{557} + 1204x^{557}y^{602}. \end{aligned}$$

$$\begin{aligned} s_x s_y(ST(G_1,x,y)) = {} & 82052x^{281}y^{292} + 89920x^{281}y^{320} + 80366x^{281}y^{286} + 83798x^{286}y^{293} \\ & + 89060x^{292}y^{305} + 100792x^{293}y^{344} + 89072x^{293}y^{304} + 104272x^{304}y^{343} \\ & + 100624x^{304}y^{331} + 98210x^{305}y^{322} + 108580x^{305}y^{356} + 115520x^{320}y^{361} \\ & + 114954x^{322}y^{357} + 116242x^{322}y^{361} + 120106x^{322}y^{373} + 119160x^{331}y^{360} \\ & + 131712x^{343}y^{384} + 287028x^{357}y^{402} + 147960x^{360}y^{411} + 141480x^{360}y^{393} \\ & + 441864x^{361}y^{408} + 146566x^{361}y^{406} + 331008x^{384}y^{431} + 168204x^{393}y^{428} \\ & + 1092636x^{402}y^{453} + 183918x^{406}y^{453} + 185542x^{406}y^{457} + 556920x^{408}y^{455} \\ & + 199020x^{428}y^{465} + 412036x^{431}y^{478} + 226500x^{453}y^{500} + 227500x^{455}y^{500} \\ & + 456820x^{455}y^{502} + 474300x^{465}y^{510} + 501900x^{478}y^{525} + 572220x^{510}y^{561} \\ & + 568140x^{510}y^{557} + 670628x^{557}y^{602}. \end{aligned}$$

Journal of Chemical Health Risks

www.jchr.org

JCHR (2024) 14(3), 879-898 | ISSN:2251-6727

$$
\begin{aligned}
E_xE_y(G_1,x,y) = {} & \frac{x^{281}y^{292}}{82052} + \frac{x^{281}y^{320}}{89920} + \frac{x^{281}y^{286}}{80366} + \frac{x^{286}y^{293}}{83798} + \frac{x^{292}y^{305}}{89060} + \frac{x^{293}y^{344}}{100792} + \frac{x^{293}y^{304}}{89072} + \frac{x^{304}y^{343}}{104272} \\
& + \frac{x^{304}y^{331}}{100624} + \frac{x^{305}y^{322}}{98210} + \frac{x^{305}y^{356}}{108580} + \frac{x^{320}y^{361}}{115520} + \frac{x^{322}y^{357}}{114954} + \frac{x^{322}y^{361}}{116242} + \frac{x^{322}y^{373}}{120106} + \frac{x^{331}y^{360}}{119160} \\
& + \frac{x^{343}y^{384}}{131712} + \frac{x^{357}y^{402}}{71757} + \frac{x^{360}y^{411}}{147960} + \frac{x^{360}y^{393}}{141480} + \frac{x^{361}y^{408}}{49096} + \frac{x^{361}y^{406}}{146566} + \frac{x^{384}y^{431}}{82752} + \frac{x^{393}y^{428}}{168204} \\
& + \frac{x^{402}y^{453}}{30351} + \frac{x^{406}y^{453}}{183918} + \frac{x^{406}y^{457}}{185542} + \frac{x^{408}y^{455}}{61880} + \frac{x^{428}y^{465}}{199020} + \frac{x^{431}y^{478}}{103009} + \frac{x^{453}y^{500}}{226500} + \frac{x^{455}y^{500}}{227500} \\
& + \frac{x^{455}y^{502}}{114205} + \frac{x^{465}y^{510}}{118575} + \frac{x^{478}y^{525}}{125475} + \frac{x^{510}y^{561}}{143055} + \frac{x^{510}y^{557}}{142035} + \frac{x^{557}y^{602}}{167657}.
\end{aligned}
$$

$$
\begin{aligned}
s_x^2(ST(G_1,x,y)) = {} & 78961x^{281}y^{292} + 78961x^{281}y^{320} + 78961x^{281}y^{286} + 81796x^{286}y^{293} + 85264x^{292}y^{305} \\
& + 85849x^{293}y^{344} + 85849x^{293}y^{304} + 92416x^{304}y^{343} + 92416x^{304}y^{331} + 93025x^{305}y^{322} \\
& + 93025x^{305}y^{356} + 102400x^{320}y^{361} + 103684x^{322}y^{357} + 103684x^{322}y^{361} + 103684x^{322}y^{373} \\
& + 109561x^{331}y^{360} + 117649x^{343}y^{384} + 254898x^{357}y^{402} + 129600x^{360}y^{411} + 129600x^{360}y^{393} \\
& + 390963x^{361}y^{408} + 130321x^{361}y^{406} + 294912x^{384}y^{431} + 154449x^{393}y^{428} + 969624x^{402}y^{453} \\
& + 164836x^{406}y^{453} + 164836x^{406}y^{457} + 499392x^{408}y^{455} + 183184x^{428}y^{465} + 371522x^{431}y^{478} \\
& + 205209x^{453}y^{500} + 207025x^{455}y^{500} + 414050x^{455}y^{502} + 432450x^{465}y^{510} + 456968x^{478}y^{525} \\
& + 520200x^{510}y^{561} + 520200x^{510}y^{557} + 620498x^{557}y^{602}.
\end{aligned}
$$

$$
\begin{aligned}
s_y^2(ST(G_1,x,y)) = {} & 85264x^{281}y^{292} + 102400x^{281}y^{320} + 81796x^{281}y^{286} + 85849x^{286}y^{293} + 93025x^{292}y^{305} \\
& + 118336x^{293}y^{344} + 92416x^{293}y^{304} + 117649x^{304}y^{343} + 109561x^{304}y^{331} + 103684x^{305}y^{322} \\
& + 126736x^{305}y^{356} + 130321x^{320}y^{361} + 127449x^{322}y^{357} + 130321x^{322}y^{361} + 139129x^{322}y^{373} \\
& + 129600x^{331}y^{360} + 147456x^{343}y^{384} + 323208x^{357}y^{402} + 168921x^{360}y^{411} + 154449x^{360}y^{393} \\
& + 499392x^{361}y^{408} + 164836x^{361}y^{406} + 371522x^{384}y^{431} + 183184x^{393}y^{428} + 1231254x^{402}y^{453} \\
& + 205209x^{406}y^{453} + 208849x^{406}y^{457} + 621075x^{408}y^{455} + 216225x^{428}y^{465} + 456968x^{431}y^{478} \\
& + 250000x^{453}y^{500} + 250000x^{455}y^{500} + 504008x^{455}y^{502} + 520200x^{465}y^{510} + 551250x^{478}y^{525} \\
& + 629442x^{510}y^{561} + 620498x^{510}y^{557} + 724808x^{557}y^{602}.
\end{aligned}
$$

$$
\begin{aligned}
s_xs_y(s_x+s_y)(ST(G_1,x,y)) = {} & 47015796x^{281}y^{292} + 54041920x^{281}y^{320} + 45567522x^{281}y^{286} \\
& + 48519042x^{286}y^{293} + 53168820x^{292}y^{305} + 64204504x^{293}y^{344} \\
& + 53175984x^{293}y^{304} + 67463984x^{304}y^{343} + 63896240x^{304}y^{331} \\
& + 61577670x^{305}y^{322} + 71771380x^{305}y^{356} + 78669120x^{320}y^{361} \\
& + 78053766x^{322}y^{357} + 79393286x^{322}y^{361} + 83473670x^{322}y^{373} \\
& + 82339560x^{331}y^{360} + 95754624x^{343}y^{384} + 217854252x^{357}y^{402} \\
& + 114077160x^{360}y^{411} + 106534440x^{360}y^{393} + 339793416x^{361}y^{408} \\
& + 112416122x^{361}y^{406} + 269771520x^{384}y^{431} + 138095484x^{393}y^{428} \\
& + 934203780x^{402}y^{453} + 157985562x^{406}y^{453} + 160122746x^{406}y^{457} \\
& + 480621960x^{408}y^{455} + 177724860x^{428}y^{465} + 374540724x^{431}y^{478} \\
& + 215854500x^{453}y^{500} + 217262500x^{455}y^{500} + 437176740x^{455}y^{502} \\
& + 462442500x^{465}y^{510} + 503405700x^{478}y^{525} + 612847620x^{510}y^{561} \\
& + 606205380x^{510}y^{557} + 777257852x^{557}y^{602}.
\end{aligned}
$$

Journal of Chemical Health Risks

www.jchr.org

JCHR (2024) 14(3), 879-898 | ISSN:2251-6727

$$
\begin{aligned}
(s_xE_y + E_xs_y)(ST(G_1,x,y)) = {} & \frac{164225x^{281}y^{292}}{82052} + \frac{181361x^{281}y^{320}}{89920} + \frac{160757x^{281}y^{286}}{80366} + \frac{167645x^{286}y^{293}}{83798} \\
& + \frac{178289x^{292}y^{305}}{89060} + \frac{204185x^{293}y^{344}}{100792} + \frac{178265x^{293}y^{304}}{89072} + \frac{210065x^{304}y^{343}}{104272} \\
& + \frac{201977x^{304}y^{331}}{100624} + \frac{196709x^{305}y^{322}}{98210} + \frac{219761x^{305}y^{356}}{108580} + \frac{232721x^{320}y^{361}}{115520} \\
& + \frac{4717x^{322}y^{357}}{2346} + \frac{234005x^{322}y^{361}}{116242} + \frac{242813x^{322}y^{373}}{120106} + \frac{239161x^{331}y^{360}}{119160} \\
& + \frac{265105x^{343}y^{384}}{131712} + \frac{32117x^{357}y^{402}}{7973} + \frac{33169x^{360}y^{411}}{16440} + \frac{31561x^{360}y^{393}}{15720} \\
& + \frac{296785x^{361}y^{408}}{49096} + \frac{295157x^{361}y^{406}}{146566} + \frac{333217x^{384}y^{431}}{82752} + \frac{337633x^{393}y^{428}}{168204} \\
& + \frac{122271x^{402}y^{453}}{10117} + \frac{370045x^{406}y^{453}}{183918} + \frac{373685x^{406}y^{457}}{185542} + \frac{373489x^{408}y^{455}}{61880} \\
& + \frac{399409x^{428}y^{465}}{199020} + \frac{414245x^{431}y^{478}}{103009} + \frac{455209x^{453}y^{500}}{226500} + \frac{18281x^{455}y^{500}}{9100} \\
& + \frac{459029x^{455}y^{502}}{114205} + \frac{2117x^{465}y^{510}}{527} + \frac{504109x^{478}y^{525}}{125475} + \frac{221x^{510}y^{561}}{55} \\
& + \frac{570349x^{510}y^{557}}{142035} + \frac{672653x^{557}y^{602}}{167657}.
\end{aligned}
$$

$$
\begin{aligned}
(E_xJs_xs_y)(ST(G_1,x,y)) = {} & \frac{82052x^{573}}{573} + \frac{89920x^{601}}{601} + \frac{80366x^{567}}{567} + \frac{83798x^{579}}{579} + \frac{89060x^{597}}{597} \\
& + \frac{100792x^{637}}{637} + \frac{89072x^{597}}{597} + \frac{104272x^{647}}{647} + \frac{100624x^{635}}{635} + \frac{98210x^{627}}{627} \\
& + \frac{108580x^{661}}{661} + \frac{115520x^{681}}{681} + \frac{16422x^{679}}{97} + \frac{116242x^{683}}{683} + \frac{120106x^{695}}{695} \\
& + \frac{119160x^{691}}{691} + \frac{131712x^{727}}{727} + \frac{95676x^{759}}{253} + \frac{49320x^{771}}{257} + \frac{47160x^{753}}{251} \\
& + \frac{441864x^{769}}{769} + \frac{146566x^{767}}{767} + \frac{331008x^{815}}{815} + \frac{168204x^{821}}{821} + \frac{121404x^{855}}{95} \\
& + \frac{183918x^{859}}{859} + \frac{185542x^{863}}{863} + \frac{556920x^{863}}{863} + \frac{199020x^{893}}{893} + \frac{412036x^{909}}{909} \\
& + \frac{226500x^{953}}{953} + \frac{45500x^{955}}{191} + \frac{456820x^{957}}{957} + \frac{6324x^{975}}{13} + \frac{501900x^{1003}}{1003} \\
& + \frac{3740x^{1071}}{7} + \frac{568140x^{1067}}{1067} + \frac{670628x^{1159}}{1159}.
\end{aligned}
$$

Journal of Chemical Health Risks
www.jchr.org
JCHR (2024) 14(3), 879-898 | ISSN:2251-6727

$$(2E_xJ)(ST(G_1,x,y)) = \frac{2x^{573}}{573} + \frac{2x^{601}}{601} + \frac{2x^{567}}{567} + \frac{2x^{579}}{579} + \frac{2x^{597}}{597} + \frac{2x^{637}}{637} + \frac{2x^{597}}{597} + \frac{2x^{647}}{647} + \frac{2x^{635}}{635}$$
$$+ \frac{2x^{627}}{627} + \frac{2x^{661}}{661} + \frac{2x^{681}}{681} + \frac{2x^{679}}{679} + \frac{2x^{683}}{683} + \frac{2x^{695}}{695} + \frac{2x^{691}}{691} + \frac{2x^{727}}{727} + \frac{4x^{759}}{759}$$
$$+ \frac{2x^{771}}{771} + \frac{2x^{753}}{753} + \frac{6x^{769}}{769} + \frac{2x^{767}}{767} + \frac{4x^{815}}{815} + \frac{2x^{821}}{821} + \frac{4x^{855}}{285} + \frac{2x^{859}}{859} + \frac{2x^{863}}{863}$$
$$+ \frac{6x^{863}}{863} + \frac{2x^{893}}{893} + \frac{4x^{909}}{909} + \frac{2x^{953}}{953} + \frac{2x^{955}}{955} + \frac{4x^{957}}{957} + \frac{4x^{975}}{975} + \frac{4x^{1003}}{1003} + \frac{4x^{1071}}{1071}$$
$$+ \frac{4x^{1067}}{1067} + \frac{4x^{1159}}{1159}.$$

$$(E_xJs_xs_y)(ST(G_1,x,y)) = \frac{82052x^{281}y^{292}}{573} + \frac{89920x^{281}y^{320}}{601} + \frac{80366x^{281}y^{286}}{567} + \frac{83798x^{286}y^{293}}{579}$$
$$+ \frac{89060x^{292}y^{305}}{597} + \frac{100792x^{293}y^{344}}{637} + \frac{89072x^{293}y^{304}}{597} + \frac{104272x^{304}y^{343}}{647}$$
$$+ \frac{100624x^{304}y^{331}}{635} + \frac{98210x^{305}y^{322}}{627} + \frac{108580x^{305}y^{356}}{661} + \frac{115520x^{320}y^{361}}{681}$$
$$+ \frac{16422x^{322}y^{357}}{97} + \frac{116242x^{322}y^{361}}{683} + \frac{120106x^{322}y^{373}}{695} + \frac{119160x^{331}y^{360}}{691}$$
$$+ \frac{131712x^{343}y^{384}}{727} + \frac{95676x^{357}y^{402}}{253} + \frac{49320x^{360}y^{411}}{257} + \frac{47160x^{360}y^{393}}{251}$$
$$+ \frac{441864x^{361}y^{408}}{769} + \frac{146566x^{361}y^{406}}{767} + \frac{331008x^{384}y^{431}}{815} + \frac{168204x^{393}y^{428}}{821}$$
$$+ \frac{121404x^{402}y^{453}}{95} + \frac{183918x^{406}y^{453}}{859} + \frac{185542x^{406}y^{457}}{863} + \frac{556920x^{408}y^{455}}{863}$$
$$+ \frac{199020x^{428}y^{465}}{893} + \frac{412036x^{431}y^{478}}{909} + \frac{226500x^{453}y^{500}}{953} + \frac{45500x^{455}y^{500}}{191}$$
$$+ \frac{456820x^{455}y^{502}}{957} + \frac{6324x^{465}y^{510}}{13} + \frac{501900x^{478}y^{525}}{1003} + \frac{3740x^{510}y^{561}}{7}$$
$$+ \frac{568140x^{510}y^{557}}{1067} + \frac{670628x^{557}y^{602}}{1159}.$$

The formulas in Table 1 and the equations above provide the following results:

$$S_1(G_1) = (s_x + s_y)(ST(G;x,y))\big|(1,1) = 45968.$$

$$S_2(G_1) = (s_xs_y)(ST(G;x,y))\big|(1,1) = 9736630.$$

$$S_3(G_1) = (E_xE_y)(ST(G;x,y))\big|(1,1) = 0.000370867.$$

$$FS(G_1) = (s_x^2 + s_y^2)(ST(G;x,y))\big|(1,1) = 19578212.$$

$$RS(G_1) = (s_xs_y(s_x + s_y))(ST(G;x,y))\big|(1,1)$$
$$= 8544281706.$$

$$SDDS(G_1) = (s_xE_y + E_xs_y)(ST(G;x,y))\big|(1,1)$$
$$= 112.6173684.$$

$$ISSI(G_1) = (E_xJs_xs_y)(ST(G;x,y))\big|(1)$$
$$= 11460.63794.$$

$$HS(G_1) = (2E_xJ)(ST(G,x,y))\big|(1) = 0.141375317.$$

$$AS(G_1) = (E_xc_{-2}Js_x^3s_y^3)(ST(G,x,y))\big|(1)$$
$$= 534864898.3.$$

Theorem 3.1.3. Let G_2 be the chemical graph of CID89869520 structure. Then

$$ST(G_1,x,y) = \sum_{22\le 28} d_{22,28}x^{22}y^{28} + \sum_{22\le 26} d_{22,26}x^{22}y^{26} + \sum_{22\le 24} d_{22,24}x^{22}y^{24} + \sum_{24\le 26} d_{24,26}x^{24}y^{26}$$
$$+ \sum_{24\le 34} d_{24,34}x^{24}y^{34} + \sum_{26\le 28} d_{26,28}x^{26}y^{28} + \sum_{26\le 30} d_{26,30}x^{26}y^{30} + \sum_{26\le 36} d_{26,36}x^{26}y^{36}$$
$$+ \sum_{28\le 38} d_{28,38}x^{28}y^{38} + \sum_{28\le 30} d_{28,30}x^{28}y^{30}.$$

Journal of Chemical Health Risks
www.jchr.org
JCHR (2024) 14(3), 879-898 | ISSN:2251-6727

Proof. From Figure 2, it is easy to see that $|V| = 12, |E| = 12$ and also $|E_{22,28}| = 1, |E_{22,26}| = 1,$ $|E_{22,24}| = 1, |E_{24,26}| = 1, |E_{24,34}| = 1, |E_{293,344}| = 1,$ $|E_{26,28}| = 1, |E_{26,30}| = 1, |E_{26,36}| = 1, |E_{28,38}| = 1$ and $|E_{28,30}| = 1$

From the Equation (1), it is obtained

$$\begin{aligned} ST(G_1,x,y) = & \sum_{22\le 28} d_{22,28}x^{22}y^{28} + \sum_{22\le 26} d_{22,26}x^{22}y^{26} + \sum_{22\le 24} d_{22,24}x^{22}y^{24} + \sum_{24\le 26} d_{24,26}x^{24}y^{26} \\ & + \sum_{24\le 34} d_{24,34}x^{24}y^{34} + \sum_{26\le 28} d_{26,28}x^{26}y^{28} + \sum_{26\le 30} d_{26,30}x^{26}y^{30} + \sum_{26\le 36} d_{26,36}x^{26}y^{36} \\ & + \sum_{28\le 38} d_{28,38}x^{28}y^{38} + \sum_{28\le 30} d_{28,30}x^{28}y^{30}. \end{aligned}$$

$$\begin{aligned} ST(G_1,x,y) = & x^{22}y^{28} + x^{22}y^{26} + x^{22}y^{24} + x^{24}y^{26} + x^{24}y^{34} + x^{26}y^{28} + x^{26}y^{30} + x^{26}y^{36} + 3x^{28}y^{38} \\ & + x^{28}y^{30}. \end{aligned}$$

The chemical structure and 3D plots of the ST_p of **CID89869520** structure are displayed Figure 5.

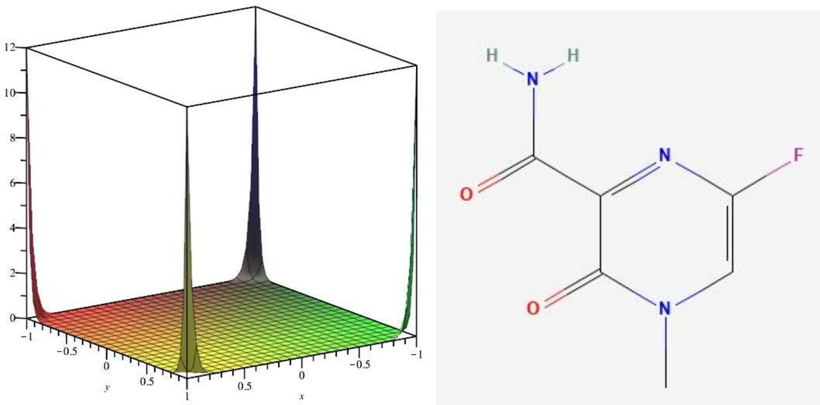

Figure 5. The chemical structure and the Plots of ST_p of **CID89869520.**

Theorem 3.1.4. The G_2 graph's various TIs are as follows:

$S_1(G_1) = 680$

$SDDS(G_1) = 24.64251034$

$S_2(G_1) = 9632\ 7.$

$ISSI(G_1) = 167.6171151$

$S_3(G_1) = 0.015827701$ $HS(G_1) = 0.430028923$

$FS(G_1) = 19848$

$AS(G_1) = 37769.3089$

$RS(G_1) = 561488$

Proof. The following equations are derived from Theorem 3.1.3:

Journal of Chemical Health Risks
www.jchr.org
JCHR (2024) 14(3), 879-898 | ISSN:2251-6727

$$s_x(ST(G_1,x,y)) = 22x^{22}y^{28} + 22x^{22}y^{26} + 22x^{22}y^{24} + 24x^{24}y^{26} + 24x^{24}y^{34} + 26x^{26}y^{28} + 26x^{26}y^{30} + 26x^{26}y^{36} + 84x^{28}y^{38} + 28x^{28}y^{30}.$$

$$s_y(ST(G_1,x,y)) = 28x^{22}y^{28} + 26x^{22}y^{26} + 24x^{22}y^{24} + 26x^{24}y^{26} + 34x^{24}y^{34} + 28x^{26}y^{28} + 30x^{26}y^{30} + 36x^{26}y^{36} + 114x^{28}y^{38} + 30x^{28}y^{30}.$$

$$s_xs_y(ST(G_1,x,y)) = 616x^{22}y^{28} + 572x^{22}y^{26} + 528x^{22}y^{24} + 624x^{24}y^{26} + 816x^{24}y^{34} + 728x^{26}y^{28} + 780x^{26}y^{30} + 936x^{26}y^{36} + 3192x^{28}y^{38} + 840x^{28}y^{30}.$$

$$E_xE_y(G_1,x,y) = \frac{x^{22}y^{28}}{616} + \frac{x^{22}y^{26}}{572} + \frac{x^{22}y^{24}}{528} + \frac{x^{24}y^{26}}{624} + \frac{x^{24}y^{34}}{816} + \frac{x^{26}y^{28}}{728} + \frac{x^{26}y^{30}}{780} + \frac{x^{26}y^{36}}{936} + \frac{3x^{28}y^{38}}{1064} + \frac{x^{28}y^{30}}{840}.$$

$$s_x^2(ST(G_1,x,y)) = 484x^{22}y^{28} + 484x^{22}y^{26} + 484x^{22}y^{24} + 576x^{24}y^{26} + 576x^{24}y^{34} + 676x^{26}y^{28} + 676x^{26}y^{30} + 676x^{26}y^{36} + 2352x^{28}y^{38} + 784x^{28}y^{30}.$$

$$s_y^2(ST(G_1,x,y)) = 784x^{22}y^{28} + 676x^{22}y^{26} + 576x^{22}y^{24} + 676x^{24}y^{26} + 1156x^{24}y^{34} + 784x^{26}y^{28} + 900x^{26}y^{30} + 1296x^{26}y^{36} + 4332x^{28}y^{38} + 900x^{28}y^{30}.$$

$$s_xs_y(s_x+s_y)(ST(G_1,x,y)) = 30800x^{22}y^{28} + 27456x^{22}y^{26} + 24288x^{22}y^{24} + 31200x^{24}y^{26} + 47328x^{24}y^{34} + 39312x^{26}y^{28} + 43680x^{26}y^{30} + 58032x^{26}y^{36} + 210672x^{28}y^{38} + 48720x^{28}y^{30}.$$

$$(s_xE_y + E_xs_y)(ST(G_1,x,y)) = \frac{317x^{22}y^{28}}{154} + \frac{290x^{22}y^{26}}{143} + \frac{265x^{22}y^{24}}{132} + \frac{313x^{24}y^{26}}{156} + \frac{433x^{24}y^{34}}{204} + \frac{365x^{26}y^{28}}{182} + \frac{394x^{26}y^{30}}{195} + \frac{493x^{26}y^{36}}{234} + \frac{1671x^{28}y^{38}}{266} + \frac{421x^{28}y^{30}}{210}.$$

$$(E_xJs_xs_y)(ST(G_1,x,y)) = \frac{308x^{50}}{25} + \frac{143x^{48}}{12} + \frac{264x^{46}}{23} + \frac{312x^{50}}{25} + \frac{408x^{58}}{29} + \frac{364x^{54}}{27} + \frac{195x^{56}}{14} + \frac{468x^{62}}{31} + \frac{532x^{66}}{11} + \frac{420x^{58}}{29}.$$

$$(2E_xJ)(ST(G_1,x,y)) = \frac{x^{50}}{25} + \frac{x^{48}}{24} + \frac{x^{46}}{23} + \frac{x^{50}}{25} + \frac{x^{58}}{29} + \frac{x^{54}}{27} + \frac{x^{56}}{28} + \frac{x^{62}}{31} + \frac{x^{66}}{11} + \frac{x^{58}}{29}.$$

$$(E_xJs_xs_y)(ST(G_1,x,y)) = \frac{456533x^{50}}{216} + \frac{23393656x^{48}}{12167} + 1728x^{46} + 2197x^{50} + \frac{1061208x^{58}}{343} + 2744x^{54} + \frac{2197000x^{56}}{729} + \frac{474552x^{62}}{125} + \frac{7057911x^{66}}{512} + 3375x^{58}.$$

The formulas in Table 1 and the equations above provide the following results:

$$S_1(G_1) = \left(s_x + s_y\right)\left(ST(G;x,y)\right)\Big|(1,1) = 680.$$

$$S_2(G_1) = \left(s_xs_y\right)\left(ST(G;x,y)\right)\Big|(1,1) = 9632.$$

$$S_3(G_1) = \left(E_xE_y\right)\left(ST(G;x,y)\right)\Big|(1,1) = 0.015827701.$$

$$FS(G_1) = \left(s_x^2 + s_y^2\right)\left(ST(G;x,y)\right)\Big|(1,1) = 19848.$$

$$RS(G_1) = \left(s_xs_y\left(s_x + s_y\right)\right)\left(ST(G;x,y)\right)\Big|(1,1) = 561488.$$

$$SDDS(G_1) = \left(s_xE_y + E_xs_y\right)\left(ST(G;x,y)\right)\Big|(1,1) = 24.64251034.$$

$$ISSI(G_1) = \left(E_xJs_xs_y\right)\left(ST(G;x,y)\right)\Big|(1) = 167.6171151.$$

$$HS(G_1) = (2E_xJ)\left(ST(G;x,y)\right)\Big|(1) = 0.430028923.$$

Journal of Chemical Health Risks
www.jchr.org
JCHR (2024) 14(3), 879-898 | ISSN:2251-6727

$AS(G_1) = \left(E_x c_{-2} J s_x^3 s_y^3\right)\left(ST(G;x,y)\right)\Big|(1) = 37769.30899.$

For all the drugs considered we now list the ST-polynomials and their plots are obtained as in the case of Theorems 3.1.1 and 3.1.3. These are listed in the following table.

Table2. ST- Polynomials and their plots for COVID -19 drugs.

Drugs and their chemical structures	**ST- polynomial and their 3D-plots**
CID10009410: 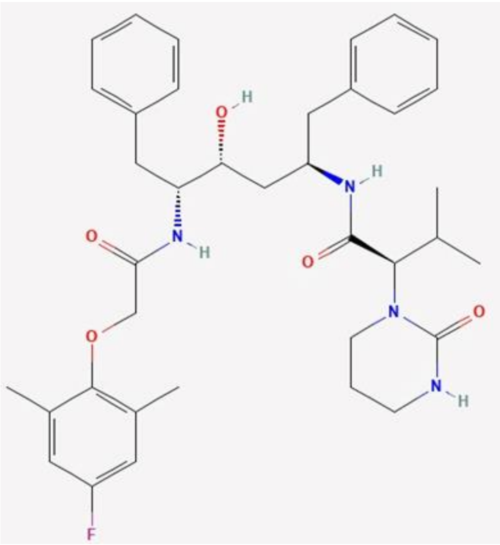	$x^{248}y^{250} + x^{248}y^{248} + x^{250}y^{268} + x^{250}y^{282} + x^{268}y^{288} + x^{282}y^{316} + x^{288}y^{312} + x^{288}y^{332} + x^{312}y^{338} + x^{312}y^{352} + x^{312}y^{344} + x^{316}y^{356} + x^{338}y^{366} + x^{344}y^{382} + x^{344}y^{384} + x^{352}y^{396} + x^{356}y^{396} + x^{366}y^{402} + x^{382}y^{426} + x^{382}y^{422} + x^{384}y^{424} + x^{396}y^{436} + x^{402}y^{440} + x^{402}y^{446} + x^{422}y^{462} + x^{424}y^{462} + x^{440}y^{476} + x^{476}y^{520}.$ 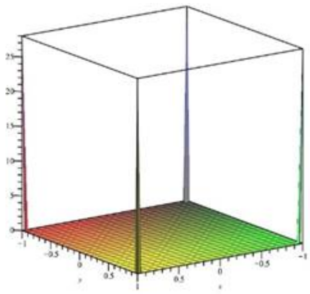
CID44271905: 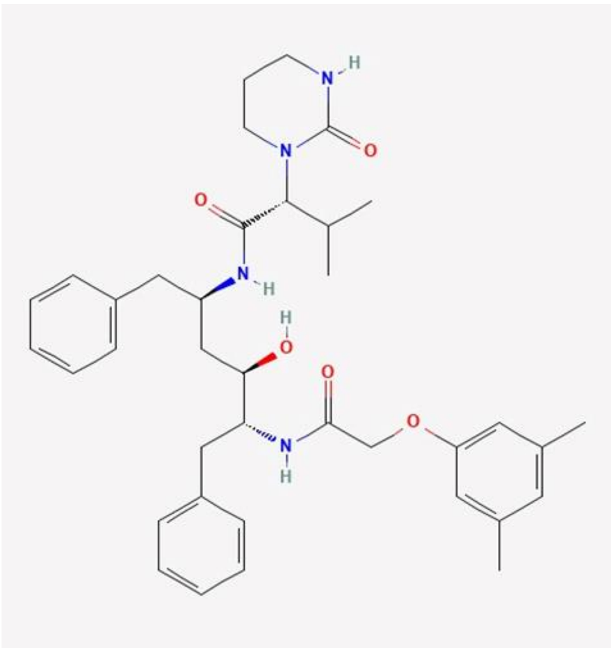	$x^{241}y^{243} + x^{241}y^{241} + x^{241}y^{285} + x^{241}y^{245} + x^{243}y^{275} + x^{243}y^{261} + x^{245}y^{277} + x^{245}y^{265} + x^{261}y^{281} + x^{265}y^{287} + x^{275}y^{309} + x^{277}y^{311} + x^{281}y^{325} + x^{281}y^{305} + x^{287}y^{331} + x^{287}y^{313} + x^{305}y^{337} + x^{305}y^{345} + x^{309}y^{349} + x^{311}y^{351} + x^{313}y^{341} + x^{337}y^{377} + x^{337}y^{375} + x^{341}y^{371} + x^{345}y^{389} + x^{349}y^{389} + x^{351}y^{391} + x^{371}y^{409} + x^{375}y^{415} + x^{375}y^{419} + x^{377}y^{417} + x^{389}y^{429} + x^{391}y^{431} + x^{409}y^{445} + x^{415}y^{455} + x^{417}y^{455} + x^{445}y^{489} + x^{445}y^{483}.$ 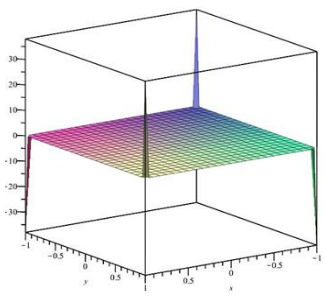

Journal of Chemical Health Risks

www.jchr.org

JCHR (2024) 14(3), 879-898 | ISSN:2251-6727

CID3010243: 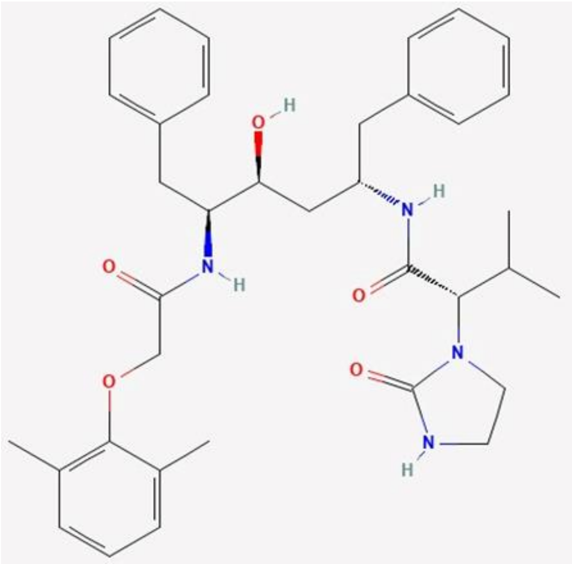	$x^{230}y^{233} + x^{230}y^{273} + x^{230}y^{231} + x^{231}y^{234} + x^{233}y^{252} + x^{233}y^{264} + x^{234}y^{265} + x^{234}y^{253} + x^{252}y^{273} + x^{253}y^{274} + x^{264}y^{297} + x^{265}y^{298} + x^{273}y^{298} + x^{273}y^{316} + x^{274}y^{317} + x^{274}y^{299} + x^{296}y^{336} + x^{297}y^{336} + x^{298}y^{325} + x^{298}y^{337} + x^{299}y^{338} + x^{299}y^{332} + x^{325}y^{354} + x^{332}y^{372} + x^{332}y^{370} + x^{335}y^{375} + x^{337}y^{376} + x^{338}y^{381} + x^{354}y^{391} + x^{370}y^{410} + x^{370}y^{413} + x^{372}y^{411} + x^{375}y^{414} + x^{376}y^{415} + x^{391}y^{430} + x^{391}y^{434} + x^{391}y^{430} + x^{410}y^{411} + x^{430}y^{467}.$ 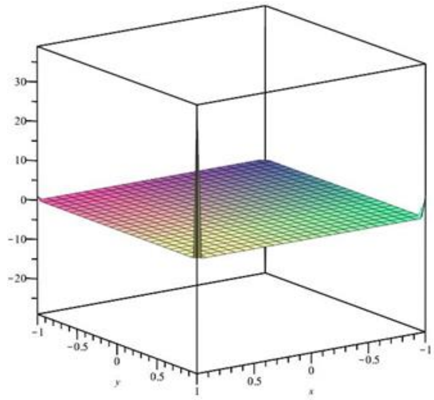
D44271958: 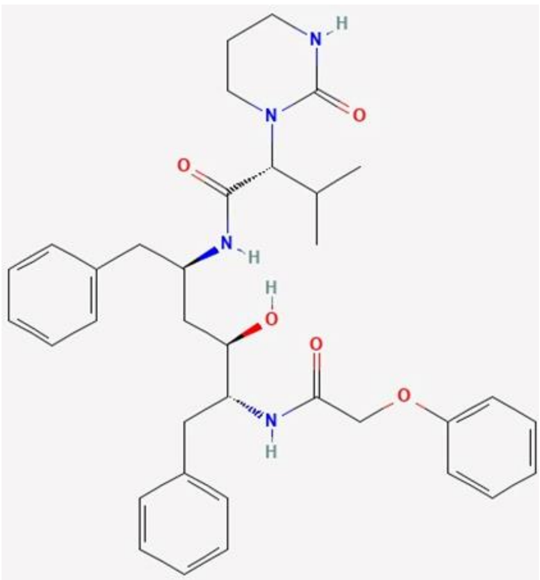	$x^{221}y^{251} + x^{221}y^{237} + x^{221}y^{221} + x^{221}y^{223} + x^{223}y^{265} + x^{223}y^{229} + x^{229}y^{259} + x^{229}y^{251} + x^{237}y^{255} + x^{251}y^{283} + x^{251}y^{275} + x^{255}y^{297} + x^{255}y^{277} + x^{259}y^{299} + x^{275}y^{317} + x^{275}y^{303} + x^{277}y^{307} + x^{277}y^{315} + x^{283}y^{321} + x^{291}y^{329} + x^{303}y^{333} + x^{307}y^{345} + x^{307}y^{343} + x^{315}y^{357} + x^{321}y^{359} + x^{329}y^{367} + x^{333}y^{365} + x^{343}y^{381} + x^{343}y^{385} + x^{345}y^{383} + x^{359}y^{397} + x^{365}y^{403} + x^{367}y^{405} + x^{381}y^{419} + x^{383}y^{419} + x^{403}y^{441} + x^{441}y^{479}.$ 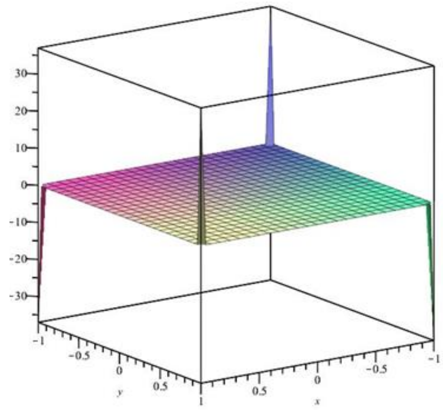

Journal of Chemical Health Risks
www.jchr.org
JCHR (2024) 14(3), 879-898 | ISSN:2251-6727

Application of topological descriptors:

We will develop a relationship between topological descriptors and the COVID-19 drugsEnthalpy of vaporization (E), flash point (FP), molar refraction (MR), polarizability (P), surface tension (T), and molar volume (MV)in this section. The different Topological indices are obtained from ST_p using Theorem 3.1.1, 3.1.3 and Table 2 which are presented in Table 3.

For each plot, we performed polynomial fitting in order to generate an equation. Table 5 shows the adjusted R^2 value for each plot. Fordrugs E, F, MR, P, T and MV it can be shown that SDDS have the best values.The highest value of adj. R^2 ensures the best fit for the data and, as a result, the equation produced from it has the least amount of inaccuracy.

Table 4 shows the experimental values for the physical and chemical characteristics of selected COVID -19 drugs.

Table 3. Topological indices derived from ST- Polynomial of COVID -19 drugs.

Drugs	Topological Descriptors								
	S_1	S_2	S_3	F	RS	SDDS	ISSI	HS	AS
CID71749833	45968	9736630	0.00037	19578212	8544281706	112.617	11460.638	0.1414	534864898.34
CID89869520	680	9632	0.01583	19848	561488	24.643	167.617	0.43003	37769.31
CID10009410	34922	6407768	0.00043	12878636	4852309120	98.479	8709.062	0.1423	304196201.26
CID44271905	34252	6184775	0.00045	12433442	4624232876	98.515	8540.683	0.1456	289873271.46
CID3010243	32060	5521148	0.00048	11101256	3929180860	96.521	7993.424	0.1491	246360882.12
CID44271958	30142	5006351	0.00052	10069606	3457674422	94.552	7513.713	0.1524	216793489.60

Table 4. COVID -19 drugs and their properties.

Drugs PubChem ID	E	FP	MR	P	T	MV
CID71749833	140.8	512.7	179.2	71	49.5	540.5
CID89869520	141.1	513.7	179.2	71	49	544.7
CID10009410	140.8	512.7	179.2	71	49.5	540.5
CID44271905	140	509.5	174.6	69.2	50.5	522.7
CID3010243	138.9	505.1	169.5	67.2	50.9	507.9
CID44271958	63.2	185.5	41.3	16.4	72.9	110

Table 5. The adj. R^2 values for the fitted curve of topological descriptors against COVID-19 properties.

Topological Descriptor	**E**	**FP**	**MR**	**P**	**T**	**MV**
S_1	0.9676	0.9676	0.9656	0.9657	0.9586	0.9628
S_2	0.9392	0.9391	0.9389	0.9389	0.9292	0.9355
S_3	0.572	0.832	0.8652	0.8647	0.8555	0.8682
FS	0.9394	0.9393	0.939	0.9391	0.9294	0.9357
RS	0.902	0.9018	0.9035	0.9035	0.8914	0.8997
SDDS	**1**	**1**	**0.9988**	**0.9988**	**0.9979**	**0.998**
ISSI	0.9674	0.9674	0.9655	0.9655	0.9584	0.9626

Journal of Chemical Health Risks
www.jchr.org
JCHR (2024) 14(3), 879-898 | ISSN:2251-6727

HS	0.9892	0.9891	0.9893	0.9893	0.9867	0.9884
AS	0.9021	0.9019	0.9036	0.9036	0.8915	0.8998

QSPR modelling shows that SDDS is best predictive Topological indices for E, F, MR, P, T and MV. Figures (Figure 6, Figure 7, Figure 8, Figure 9, Figure 10 and Figure 11) show their plots.

The Equations obtained between SDDS index against Enthalpy as follows

$$E = a + b_1 SDDS + b_2 SDDS^2 + b_3 SDDS^3 + b_4 SDDS^4 \text{ - - - - - } (2)$$

Where a =199210.8982, $b_1 = -13927.5157$, $b_2 = 294.5291$, $b_3 = -2.5055$, $b_4 = 0.0075$.

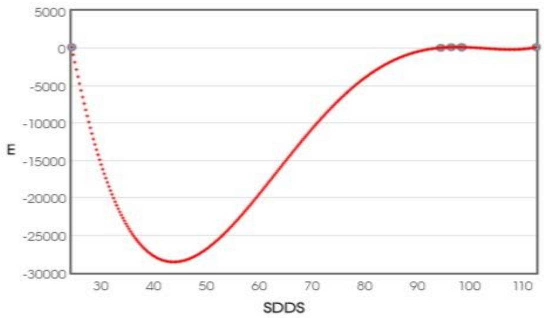

Figure 6. Curve fitting of Enthalpy against SDDS index.

The Equations obtained between SDDS index against Flash point as follows

$$FP = a + b_1 SDDS + b_2 SDDS^2 + b_3 SDDS^3 + b_4 SDDS^4 \text{ - - - - - } (3)$$

Where a =841958.915, $b_1 = -58870.427$, $b_2 = 1244.9656$, $b_3 = -10.5908$, $b_4 = 0.0319$.

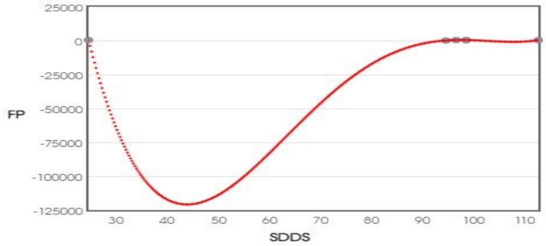

Figure 7. Curve fitting of Flash point against SDDS index.

The Equations obtained between SDDS index against Molar Refraction as follows

$$MR = a + b_1 SDDS + b_2 SDDS^2 + b_3 SDDS^3 + b_4 SDDS^4 \text{ - - - - - } (4)$$

Where a =322997.2742, $b_1 = -22579.4018$, $b_2 = 477.266$, $b_3 = -4.0579$, $b_4 = 0.0122$.

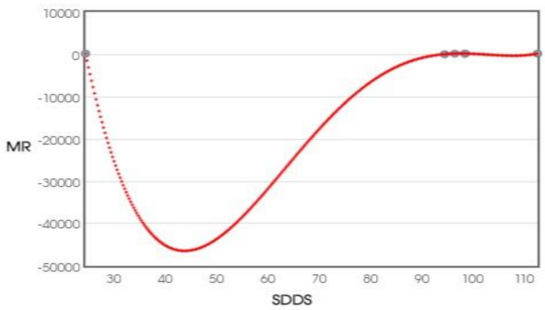

Figure 8. Curve fitting of Molar Refraction against SDDS index.

The Equations obtained between SDDS index against Polarization as follows

$$P = a + b_1 SDDS + b_2 SDDS^2 + b_3 SDDS^3 + b_4 SDDS^4 \text{ - - - - - } (4)$$

Where a =128084.4592, $b_1 = -8953.8994$, $b_2 = 189.2622$, $b_3 = -1.6092$, $b_4 = 0.0048$.

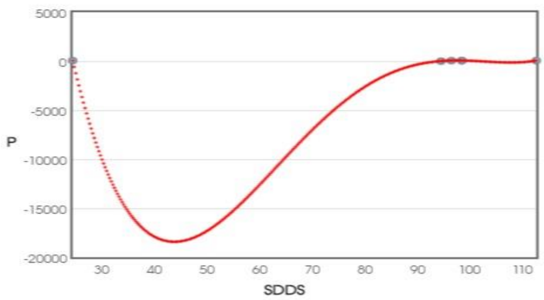

Figure 9. Curve fitting of Polarization against SDDS index.

The Equations obtained between SDDS index against Surface Tension as follows

Journal of Chemical Health Risks
www.jchr.org
JCHR (2024) 14(3), 879-898 | ISSN:2251-6727

$$T = a + b_1 SDDS + b_2 SDDS^2 + b_3 SDDS^3 + b_4 SDDS^4 - - - - - (5)$$

Where a =-56510.4643, $b_1 = 3956.5256$, $b_2 = -83.6491$, $b_3 = 0.7114$, $b_4 = -0.0021$.

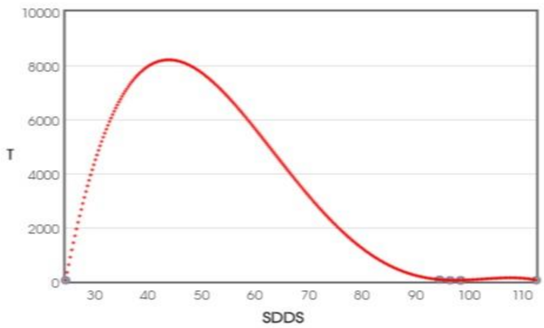

Figure 10. Curve fitting of Surface Tension against SDDS index.

The Equations obtained between SDDS index against Molar Volume as follows

$$MV = a + b_1 SDDS + b_2 SDDS^2 + b_3 SDDS^3 + b_4 SDDS^4 - - - - - (6)$$

Where a =100814.8225, $b_1 = -69962.752$, $b_2 = 1478.7889$, $b_3 = -12.573$, $b_4 = 0.0378$.

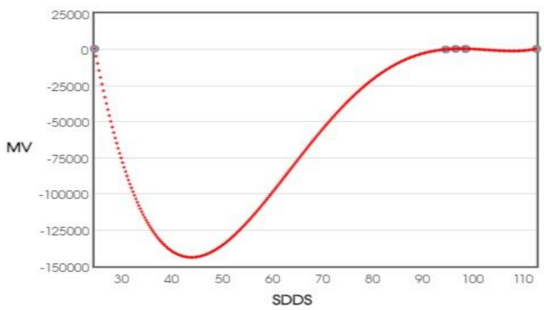

Figure 11. Curve fitting of Surface Tension against SDDS index.

The values of SDDS topological descriptor can be used to compute the E, F, MR, P, T and MV of COVID- 19 drugs, as shown by equations (2) to (8). These Eight equations make it easy for us to do so.

Conclusion

From Table 5, It is clear that most of the physio-chemical features of the medications used to treat COVID -19 may be predicted using the proposed indices. Hence, we observe that

- Enthalpy can be predicted using $S_1, S_2, FS, RS, ISSI, AS$ as the corresponding adj. R^2 values are 0.9676, 0.9392, 0.833, 0.9394, 0.902, 1, 0.9674, 0.9892 and 0.9021 respectively. Among these, we see that SDDS index is the best suited for predicting Enthalpy.
- Flash point can be predicted using $S_1, S_2, S_3, FS, RS, ISSI, AS$ as the corresponding adj. R^2 values are 0.9676, 0.9391, 0.832, 0.9393, 0.9018, 1, 0.9674, 0.9891 and 0.9019 respectively. We can see that SDDS index is the one of these that is most effective at predicting the Flash point.
- Molar Refraction can be predicted using $S_1, S_2, S_3, FS, RS, SDDS, ISSI, HS, AS$ as the corresponding adj. R^2 values are 0.997, 0.9947, 0.9582, 0.9947, 0.9919, 0.9972, 0.997, 0.9651 and 0.992 respectively. We observe that the SDDS index among these is most effective at estimating Molar Refraction.
- Polarization can be predicted using $S_1, S_2, FS, RS, SDDS, ISSI, HS, AS$ as the corresponding adj. R^2 values are 0.9657, 0.9389, 0.8647, 0.9391, 0.9035, 0.9988, 0.9655, 0.9893 and 0.9036 respectively. Among these, we can see that the SDDS index performs the task of identifying Polarization the best.
- Surface Tension can be predicted using $S_1, S_2, FS, RS, ISSI, AS$ as the corresponding adj. R^2 values are 0.9586, 0.9292, 0.8555, 0.9294, 0.8914, 0.9979, 0.9584, 0.9867 and 0.8915 respectively. We can see that the SDDS index is the one that can predicts Surface Tension the best out of all of these.
- Molar Volume can be predicted using $S_1, S_2, FS, RS, SDDS, ISSI, HS, AS$ as the corresponding adj. R^2 values are 0.9628, 0.9355, 0.8682, 0.9357, 0.8997, 0.998, 0.9626, 0.9884 and 0.8998 respectively. We can observe that among

these, the SDDS index performs the best at predicting Molar Volume.

Numerous academics have investigated the topological indices' effects on the qualities of anti-covid medicines. The best study on some anti-covid medications chosen with TIs is this one. These particular medications are now regarded as crucial in the management of COVID -19. The findings of this study will help advance the chemistry, pharmaceutical science, and most critically, the treatment of COVID-19.

Acknowledgment

The authors extend their appreciation to the Deanship of Scientific Research at King Khalid University for funding this work through Larg Groups Project under grant number (R.G.P.2/163/44).

Availability of Data and Materials

All data generated or analysed during this study are included in this published article.

Refrences

1. B. Figuerola, C. Avila, The phylum bryozoa as a promising source of anticancer drugs, Mar. Drugs, 17 (2019), 477. https://doi.org/10.3390/md17080477
2. G. Genovese, A. K. Kähler, R. E. Handsaker, J. Lindberg, S. A. Rose, S. F. Bakhoum, et al., Clonal hematopoiesis and blood-cancer risk inferred from blood DNA sequence, New Eng. J. Med., 371 (2014), 2477-2487. https://doi.org/10.1056/NEJMoa1409405
3. T. Terwilliger, M. J. B. C. J. Abdul-Hay, Acute lymphoblastic leukemia: A comprehensive review and 2017 update, Blood Cancer J., 7 (2017), e577-e577. https://doi.org/10.1038/bcj.2017.53
4. S. M. Hosamani, D. Perigidad, S. Jamagoud, Y. Maled, S. Gavade, QSPR anlysis of certain degree based topological indices, J. Statis. Appl. Prob., 6 (2017), 1-11. https://doi.org/10.18576/jsap/060211
5. M., Adnan, S. A. U. H. Bokhary, G. Abbas, T. Iqbal, Degree-based topological indices and QSPR analysis of antituberculosis drugs, J. Chem., 2022, Article ID 5748626. https://doi.org/10.1155/2022/5748626
6. J. Liu, M. Arockiaraj, M. Arulperumjothi, S. Prabhu, Distance based and Bond additive topological indices of certain repurposed antiviral drug compounds tested for treating COVID19, Int. J. Quantum Chem., 121 (2021), e26617. https://doi.org/10.1002/qua.26617
7. H. Zhang, F. Zhang, The Clar covering polynomial of hexagonal systems I, 69(1996) 147-167.
8. E.J. Farrell, An introduction to matching polynomials, Journal of Combinatorial Theory, Series B, 27(1979), 75-86.
9. F. Hassani, Ali Iranmanesh, SamanehMirzaie, Schultz and Modified Schultz Polynomials of C100 Fullerene, MATCH Commun. Math. Comput. Chem. 69 (2013) 87-92.
10. T. Doslic, Planar polycyclic graphs and their Tutte polynomials, Journal of Mathematical Chemistry, 51, (2013)1599-1607
11. D.B. West. An Introduction to Graph Theory. PrenticeHall. (1996).
12. E. Deutsch, S. Klavžar, Computing Hosoya polynomials of graphs from primary subgraphs, MATCH Commun. Math. Comput. Chem. 70 (2013) 627-644.
13. M. Eliasi, A. Iranmanesh, Hosoya polynomial of hierarchical product of graphs, MATCH Commun. Math. Comput. Chem. 69 (2013)111-119.
14. H. Hosoya, On some counting polynomials in chemistry, Discrete Appl. Math. 19 (1988)239-257.
15. X. Lin, S.J. Xu, Y.N. Yeh, Hosoya polynomials of Circumcoronene series, MATCH Commun. Math. Comput. Chem. 69 (2013)755-763.
16. M. Alaeiyan, A. Bahrami and M.R. Farahani. Cyclically Domination Polynomial of Molecular Graph of Some Nanotubes. Digest Journal of Nanomaterials and Biostructures. 6(1) (2011)143-147.
17. A.C.Bartlett, C.V.Hollot, Huang Lin, Root locations of an entire polytope of polynomials: it suffices to check the edges, Math. Control Signals Systems, 1(1988)61- 71.
18. J.I. Brown, K. Dilcher, R.J. Nowakowski, Roots of independence polynomials of well-covered graphs, J. Algebraic Combinatorics, 11 (2000)197-210.
19. J.I. Brown, C.A. Hickman and R.J. Nowakowski, On the location of roots of independence polynomials, J. Algebr. Comb., 19: 273-282 (2004).
20. J.I. Brown and R. Nowakowski, Average independence polynomials, J. Combinatorial Theory, Ser. B, 93 (2005)313- 318.
21. J.I. Brown, R. Nowakowski, Bounding the roots of independence polynomials, Ars Combinatorica, 58 (2001)113-120.

22. D.C. Fisher, A.E. Solow, Dependence polynomials, Discrete Math., 82 (1990)251-258.
23. I. Gutman, Some analytic properties of the independence and matching polynomials, MATCH Commun. Math.Comput. Chem., 28 (1992)139-150.
24. C. Hoede, X. Li, Clique polynomials and independent set polynomials of graphs, Discrete Mat. 25 (1994)219-228.
25. S. Klavzar, E. Deutsch. M-Polynomial and Degree-Based Topological Indices, Iranian Journal of Mathematical Chemistry, 6(2)(2015) 93-102.
26. F. Harary, Status and contrastatus, Sociometry, 22 (1959) 23 - 43.
27. H. S. Ramane, A. S. Yalnaik.Bounds for the status connectivity index of line graph, Int. J. Comput. Appl. Math. 12(2016) 305-310.
28. H. S. Ramane, A. S. Yalnaik, status connectivity indices of graphs and its applications to the boiling point of benzenoid hydrocarbons, Journal of Applied Mathematics and Computing, 55 (2017) 609-627.
29. H.S. Ramane, B. Basavanagoud, A.S. Yalnaik, Harmonic status index of graphs, Bulletin of Mathematical Sciences and Application, 17 (2016) 24 - 32.
30. H.S. Ramane, A.S. Yalnaik, R. Sharafdini, Status connectivity indices and coindices of graphs and its computation to some distance - balanced graphs, AKCE International Journal of graphs and combinatories, 17 (2020) 98-108.
31. K. Pattabiraman, A.Santhakumar, Second status-conncetivity indices and its coindices of composite graphs, Int. J. Math. Combin. 2(2019) 104-113.
32. K. Pattabiraman, A.Santhakumar, Bounds on hyper-status conncetivity index of graphsTWMS J. App. and Eng. Math. 11(2021) 216-227.
33. H. Wiener, Structural Determination of Paraffin Boiling Points. J. Am. Chem. Soc. 69: (1947)17-19.
34. M.C.Shanmukha, N.S.Basavarajappa, K.C.Shilpa, A.Usha, Degree-based topological indices on anticancer drugs with QSPR analysis, Heliyon, 6(6)(2020) e04235.
35. W. Gao, W. Wang, M.R. Farahani, Topological Indices Study of Molecular Structure in Anticancer Drugs, Journal of Chemistry, Volume 2016 |Article ID 3216327 | https://doi.org/10.1155/2016/3216327
36. O.C. Havare,Topological indices and QSPR modeling of some novel drugs used in the cancer treatment, Int. J.Qutum. Chem. 121(24) **(**2021) e26813, https://doi.org/10.1002/qua.26813
37. S.A. U. Bokhary, M. Adnan, M.K. Siddiqui, M. Cancan, OnTopological Indices and QSPR Analysis of Drugs Used for the Treatment of Breast Cancer, Polycyclic Aromatic Compounds, 2021, https://doi.org/10.1080/10406638.2021.1977353.
38. M. Cancan,S. Ediz,M.R. Farahani, On ve-degree atom-bond connectivity, sum-connectivity, geometric-arithmetic and harmonic indices of copper oxide. Eurasian Chem. Commun. 2 (2020) 641-645. https://doi.org/10.33945/SAMI/ECC.2020.5.11
39. M. Cancan, S. Ediz, M.Alaeiyan, M.R. Farahani, On Ve-degree molecular properties of copper oxide. Journal of Information and Optimization Sciences, 41(4),2020,949-957. https://doi.org/10.1080/02522667.2020.1747191
40. S. Ediz, M. Cancan, M. Alaeiyan, M.R. Farahani. Ve-degree and Ev-degree topological analysis of some anticancer drugs. Eurasian Chemical Communications. 2(8), 2020, 834-840. https://doi.org/10.22034/ECC.2020.107867
41. W. Gao, M.R. Farahani, S. Wang, M.N. Husin. On the edge-version atom-bond connectivity and geometric arithmetic indices of certain graph operations. Applied Mathematics and Computation 308(1), 11-17, 2017. https://doi.org/10.1016/j.amc.2017.02.046
42. H. Wang, J.B. Liu, S. Wang, W. Gao, S. Akhter, M. Imran, M.R. Farahani. Sharp bounds for the general sum-connectivity indices of transformation graphs. Discrete Dynamics in Nature and Society 2017. Article ID 2941615. https://doi.org/10.1155/2017/2941615
43. W. Gao, M.K. Jamil, A Javed, M.R. Farahani, M. Imran. Inverse sum indeg index of the line graphs of subdivision graphs of some chemical structures. UPB Sci. Bulletin B 80 (3), 97-104, 2018.
44. S Akhter, M. Imran, W. Gao, M.R. Farahani. On topological indices of honeycomb networks and graphene networks. Hacettepe Journal of Mathematics and Statistics 47 (1), 19-35, 2018.
45. X. Zhang, X. Wu, S. Akhter, M.K. Jamil, J.B. Liu, M.R. Farahani. Edge-version atom-bond connectivity and geometric arithmetic indices of generalized bridge molecular graphs. Symmetry 10 (12), 751, 2018. https://doi.org/10.3390/sym10120751

46. H. Yang, A.Q. Baig, W. Khalid, M.R. Farahani, X. Zhang. M-polynomial and topological indices of benzene ring embedded in P-type surface network. Journal of Chemistry 2019, Article ID 7297253, https://doi.org/10.1155/2019/7297253
47. D.Y. Shin, S. Hussain, F. Afzal, C. Park, D. Afzal, M.R. Farahani. Closed formulas for some new degree based topological descriptors using Mpolynomial and boron triangular nanotube. Frontiers in Chemistry, 1246, 2021. https://doi.org/10.3389/fchem.2020.613873
48. M. S. Sardar, S.-J. Xu, M. Cancan, M.R. Farahani, M. Alaeiyan, S.V. Patil. Computing Metric Dimension of Two Types of Claw-free Cubic Graphs with Applications. Journal of Combinatorial Mathematics and Combinatorial Computing. 2024, 119: 163-174. https://doi.org/10.61091/jcmcc119-17
49. A.A. Mughal, R.N. Jamil, M.R. Farahani, M. Alaeiyan, M. Cancan. Choosing Friends in Everyday Life by using Graph Theory. Journal of Combinatorial Mathematics and Combinatorial Computing. 2024, 119: 113-119. https://doi.org/10.61091/jcmcc119-12